FLIP BUCKET WITHOUT AND WITH DEFLECTORS

By Roman Juon[1] and Willi H. Hager,[2] Fellow, ASCE

ABSTRACT: Flip buckets are commonly used to discharge flow away from a hydraulic structure into a plunge pool to dissipate energy. In the past, flip buckets have often been designed in accordance with site-related hydraulic model studies. Consequently, limited generalized design guidelines are available. The present study considers flip buckets either in a prismatic rectangular channel or extended by a lateral deflector resulting in a curved jet trajectory. The main features of flip buckets are investigated, including scale effects in hydraulic models, bucket pressure distribution, and nappe trajectories with and without the presence of deflectors. An analysis is presented mainly involving the approach Froude number, the so-called bend number, and the bucket takeoff angle. It is demonstrated that the near field of a bucket-deflected jet follows the conventional parabola of a mass point, provided that the takeoff angle is correctly accounted for and that the flow is scaled using the Froude similarity law. Furthermore, shock-wave features for a flip bucket with a deflector are specified, and the governing choking relations are derived based on an experimental approach.

INTRODUCTION

Flip buckets are used when energy has to be dissipated for a flow velocity larger than about 15–20 m/s (Vischer and Hager 1998). Currently, thousands of flip buckets of various geometries involving a wide range of deflection angles, takeoff angles, relative curvature, and special elements such as teeth or banking elements are in operation. However, there has been limited standardization for flip buckets, and few design guidelines are available. In the present study, a circular-arc bucket in a prismatic rectangular channel was initially considered. The approach channel was horizontal, such as for a bottom outlet to avoid complications with steeply sloping chute flows. This flip bucket also had no curvature in plan, or banking of the invert. The first part of the study thus relates to 2D flip-bucket flow.

In the second part of the study, a simple deflector element was added to the bucket to direct flow slightly off the channel axis. Such devices have been proposed in the past [e.g., Gong et al. (1987) for the flaring gate pier, or Zhenlin et al. (1988) for the slit-type flip-bucket]. The symmetrically arranged wedge-shaped deflectors contract the flow on both sides as it leaves the bucket thus promoting air entrainment and dispersion of the flow. This Chinese proposal was not hydraulically described, nor were prototype observations provided allowing for a sound hydraulic design. This study aims to evaluate the features of the deflector extended flip bucket in the near takeoff field. Surface tension leads to scale effects that prevent far-field evaluation. Air entrainment was not studied in this project because of scaling limitations.

An important feature of flip-bucket operation not generalized until today is choking (i.e., the breakdown of supercritical bucket flow due to the presence of the bucket). The approach flow to the bucket is then subcritical and comparable to that over a low-head spillway, with a jet trajectory that is almost vertical at impact and causes significant scour at the base of the dissipator. Such flows are dangerous when not properly accounted for in the design stage because of hydraulic jumps that may submerge a bottom outlet. A generalized choking diagram is also introduced in the present study.

[1]Grad. Student; formerly, VAW-Zentrum, Eidgenössische Technische Hochschule, CH-8092 Zurich, Switzerland.

[2]Prof., Head Hydr. Div., VAW-Zentrum, Eidgenössische Technische Hochschule, CH-8092 Zurich, Switzerland.

Note. Discussion open until April 1, 2001. To extend the closing date one month, a written request must be filed with the ASCE Manager of Journals. The manuscript for this paper was submitted for review and possible publication on September 24, 1999. This paper is part of the ***Journal of Hydraulic Engineering***, Vol. 126, No. 11, November, 2000. ©ASCE, ISSN 0733-9429/00/0011-0837–0845/$8.00 + $.50 per page. Paper No. 21914.

LITERATURE REVIEW

Ski jumps were successfully introduced in France on the Dordogne hydraulic scheme, as early as the mid-1930s (Godon 1936; Coyne 1944, 1951; Auroy 1951) with detailed prototype observations conducted on the jet flow by Maitre and Obolensky (1954). Rhone and Peterka (1959) studied an improved design of flip buckets implemented by the U.S. Bureau of Reclamation (Peterka 1983).

Pressures on buckets were computed and observed by Balloffet (1961). Using a potential flow model (i.e., concentric streamlines in the bucket), he found that the maximum pressure head is on average 4% larger than computed provided the ratio of flow depth h_o in the bucket to its radius R of curvature is relatively small. Henderson and Tierney (1963) demonstrated that, for small ratio h_o/R of the potential vortex approach, the 2D computation and observations agree provided the deflection angle is at least 45°. Chen and Yu (1965) computed the pressure distribution along a cylindrical bucket by using the potential flow equations for deflection angles of β = 75° and 95°. The maximum pressure heads are close to those of Balloffet's approach.

Lenau and Cassidy (1969) improved the approach of Chen and Yu (1965). They demonstrated that the effect of viscosity in bucket flow is insignificant. The effect of gravity is important, however, involving the parameter $Q/(2gH)^{1/2}R$, where Q = discharge, and H = energy head. Because the static head is small compared to the dynamic head $V^2/2g$, one may also express their term as h_o/R. Moreover, their dimensionless pressure $p/(\rho gH)$, where g = gravitational acceleration, and ρ = fluid density, may be expressed as $p/(\rho V^2/2)$. If the pressure head is related to the approach flow depth h_o, one would have $p/(\rho V^2/2) = (1/2)[p/(\rho g h_o)] \cdot [\mathsf{F}_o^{-2}]$, where $\mathsf{F}_o = V/(gh_o)^{1/2}$ is the bucket Froude number. Maximum pressure thus depends on relative bucket curvature h_o/R and bucket Froude number $\mathbf{F}_o$. In the following, a simple combination of the two parameters is presented.

Rajan and Shivashankara Rao (1980) summarized prototype findings on ski jump flow. A common design standard is described as follows:

- Cylindrical bucket shape
- Flip angle between 20° and 40°
- Bucket height to bucket radius of the order 10^{-1}
- Bucket radius as a function of specific discharge and bucket velocity
- Bucket lip designed against cavitation damage
- Tailwater elevation well below bucket

Another summary of guidelines was also presented by Mason (1993). His additional recommendations are as follows:

J. Hydraul. Eng. 2000.126:837-845.

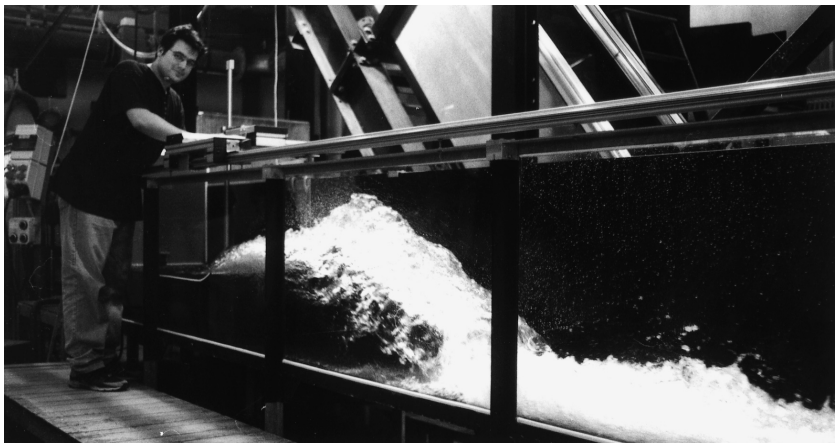

FIG. 1. Downstream View against Flip Bucket with 20° Deflector

- Minimum bucket radius three to five times the approach flow depth
- Maximum pressure according to (2), with $\sigma = 1$
- Free board of side walls by accounting for the air-water flow bulkage
- Lip angle or takeoff angle between 20° and 35°
- Spread angle of jet in air about 5°
- Splitter teeth not recommended because of cavitation risk
- Scour characteristics not considered.

These considerations were also summarized by Vischer and Hager (1995) and accounted for in the design of the present model study.

EXPERIMENTS

Experimental Facilities

The hydraulic experiments were conducted in a 499-mm-wide and 700-mm-deep rectangular channel with a total length of 7 m. The channel had a PVC invert and right wall, and a left glass wall. The flip bucket consisted of a 1-m-long approach channel with a bucket of radius R and deflection angle β. The approach channel was inserted 250 mm above the original channel invert. The discharge was controlled by a jet-box where the average flow velocity and the flow depth h_o could be independently varied in a wide range of approach Froude numbers, and excellent flow conditions resulted in terms of uniformity of flow, shock wave development due to minor perturbations of the high-speed flow, and velocity concentrations. Fig. 1 shows a view of the experimental installation.

The flip bucket contained circular arc-shaped inverts of radii R = 200 and 250 mm with a deflection angle $\beta = 30°$. Their downstream crests were sharp and located by $w + h_s$ above the downstream channel invert, where $w = (1 - \cos \beta)R$ = bucket elevation and h_s = 250 mm = elevation difference between approach and downstream channels (Fig. 2). The approach channel and the flip bucket contained 2-mm-diameter bottom pressure tappings. They were connected with a manometer battery of ± 0.5 mm reading accuracy, and pressure heads were typically read to the nearest millimeter due to turbulent fluctuations.

Linear deflectors with deflector angles $\varphi = 10°$, 20°, and 30° were also considered in this study, in addition to the prismatic flip bucket ($\varphi = 0°$). The deflector always started at the beginning of the flip bucket and ended at its downstream crest. The transitions between approach channel and deflectors were carefully finished to avoid shock-wave development at protruding corners.

A point gauge was used to determine the axial free surface approach profiles to ± 0.5 mm and the lower and upper nappe profiles for the jet discharged by the flip bucket typically to ± 1 mm. The discharge was measured with standard weirs. For $Q < 25$ L/s, a V-notch weir was used, and a rectangular thin-crested weir was installed for larger discharges up to $Q = 150$ L/s, with a reading accuracy of $\pm 1\%$. For the bucket with the deflectors, the wall profiles were also measured.

Scale effects were evaluated for the flip bucket without the deflector. Fig. 3 shows the results of preliminary observations relating to the upper nappe profile $Z'(X')$, where $X' = x/h_o$ is

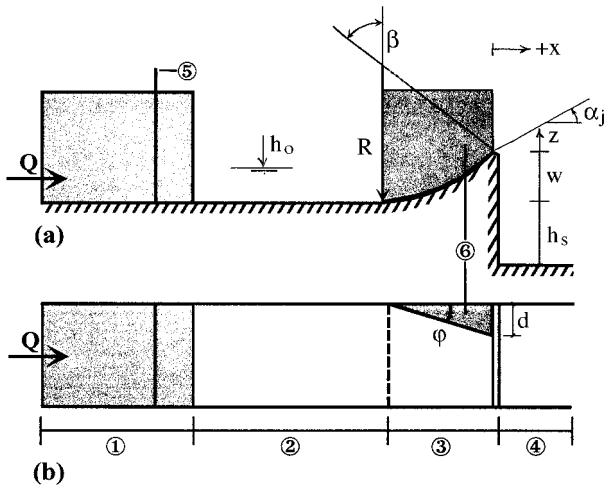

FIG. 2. Schematic View of Experimental Setup: (a) Side View; (b) Plan (with Notation as Follows: ① Jetbox, ② Approach Channel, ③ Flip-Bucket, ④ Downstream Channel, ⑤ Start of Chute, ⑥ Deflector)

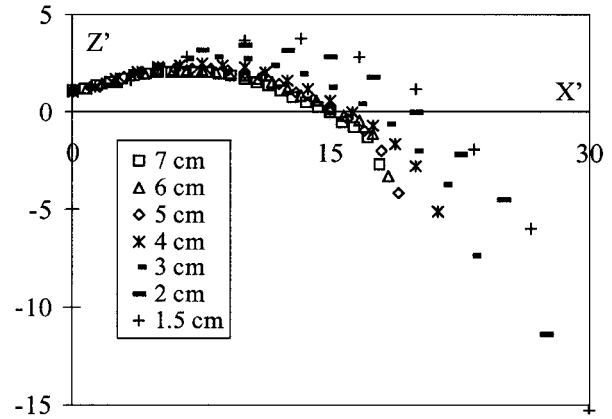

FIG. 3. Upper Nappe Profile $Z'(X')$ for $F_o = 4$ and Various Approach Flow Depths h_o

J. Hydraul. Eng. 2000.126:837-845.

the horizontal coordinate normalized with the approach flow depth, and $Z' = z/h_o$ is the corresponding vertical jet coordinate. All observations were conducted for an approach Froude number $F_o = 4$ where $F_o = V_o/(gh_o)^{1/2}$ is the approach Froude number, with $V_o = Q/(bh_o)$ = approach velocity, and g = gravitational acceleration. It may be observed in Fig. 3 that the data $Z'(X')$ follow a single curve provided $h_o \geq 5.0$ cm and that the nappe profiles deviate from this curve for smaller approach flow depths mainly due to effects of viscosity and surface tension. The limit depth $h_o \geq 5.0$ cm is in agreement with previous studies of Schwalt (1994) and Reinauer (1995) on supercritical free surface flows of water in air. In the following all experiments were conducted with $h_o \geq 5$ cm to apply the Froude similarity law for scaling up the results.

EXPERIMENTAL RESULTS

Bottom Pressure Distribution

The bottom pressure distribution along a flip bucket is a design parameter for static purposes. It is equal to the sum of the static approach pressure head h_o plus a dynamic portion. Fig. 4 shows the normalized parameter $H_P = (h_P - h_o)/(h_{PM} - h_o)$ with h_P = total pressure head and h_{PM} = maximum pressure head, plotted along the normalized streamwise coordinate $X_P = x/(R \sin \beta)$, where $x = 0$ is located at the takeoff point, and $R \sin \beta$ is the streamwise flip-bucket length. All data for the prismatic bucket ($\varphi = 0$), R = 200 and 250 mm, and $h_o \geq 5$ cm can be expressed independent of F_o as

$$H_P = [-2X_P \exp(1 + 2X_P)]^{2/3} \quad (1)$$

Note that the pressure head at $X_P = 0$ is not correctly reproduced because $h_P = 0$, but the difference is considered small for large Froude numbers $F_o > 3$. Note also that $H_P(X_P = -1) \cong 0.5$ at the bucket beginning and that there is a dynamic pressure effect upstream of the bucket. The effect of the bucket can be considered negligible for $X_P \leq -3$ because H_P is practically equal to zero.

The maximum bottom pressure head can be determined using a potential vortex model to result in $h_{PM}/h_o = (h_o/R)F_o^2$ (Vischer and Hager 1998). Accounting for the bend number $B = (h_o/R)^{0.5}F_o$ according to Vischer and Hager (1998) and σ = fitting parameter, one may write

$$h_{PM}/h_o = \sigma B^2 \quad (2)$$

Fig. 5 shows σ as a function of B, and one may note that $\sigma = 1$ for $B < 1.5$ and $\sigma = 1.3B^{-0.5}$ for larger B. The potential flow model thus agrees with observations for small B (i.e., for small relative flow depths h_o/R or small F_o) and overpredicts observations for large relative flow depths or large Froude numbers, for which the streamlines cannot be simplified with concentric circular arches. Also note the slight deviation of the data for h_o = 4 cm because of scale effects previously discussed. The pressure distribution on the sidewalls increases

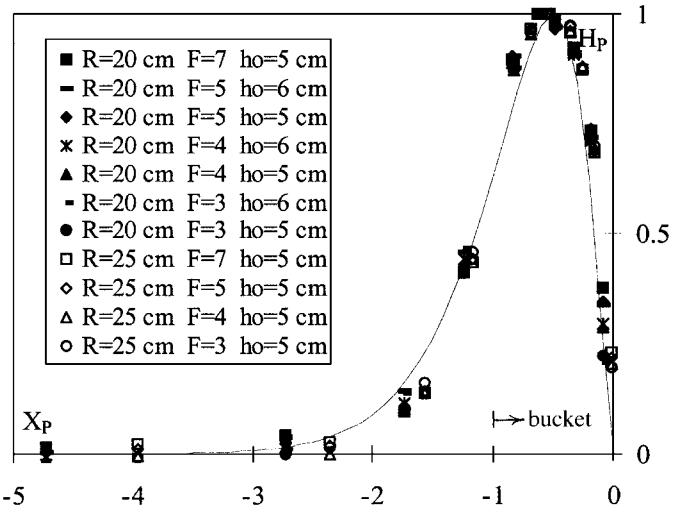

FIG. 4. Normalized Bottom Pressure Head H_P as Function of X_P [(——) Eq. (1)]

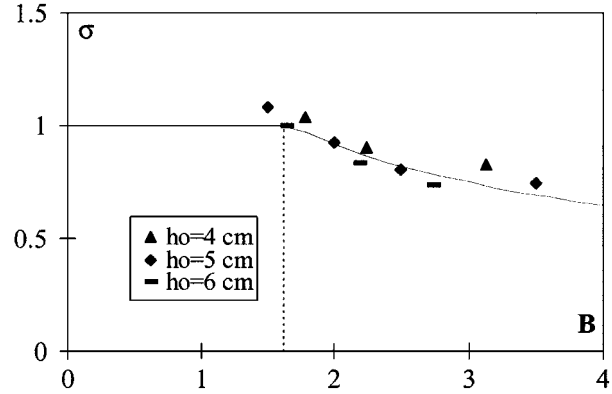

FIG. 5. Fitting Parameter σ as Function of Bend Number $B = (h_o/R)^{0.5}F_o$ for R = 200 mm

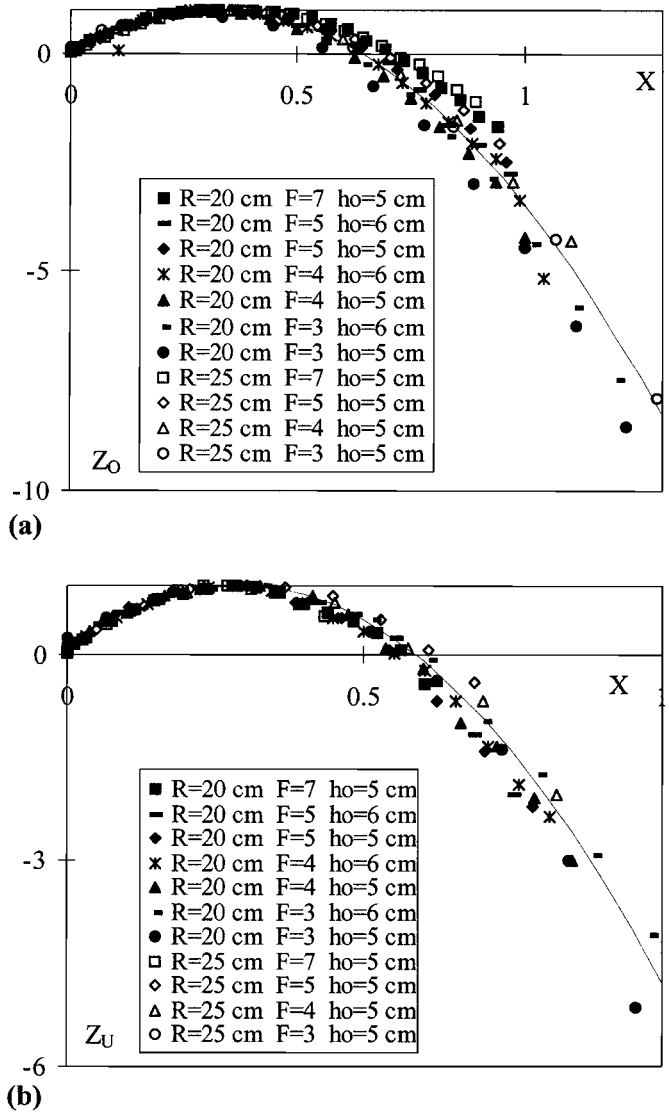

FIG. 6. (a) Upper Nappe Profile $Z_o(X)$ [(——) Eq. (4)]; (b) Lower Nappe Profile $Z_U(X)$ [(——) Eq. (4)]

J. Hydraul. Eng. 2000.126:837-845.

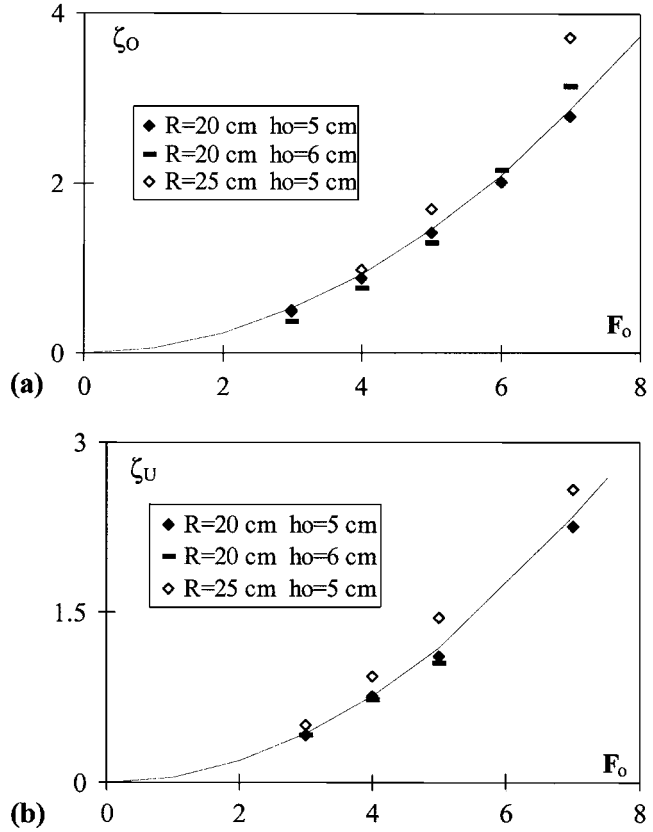

FIG. 7. Maximum Nappe Elevations as Function of F_o for: (a) Upper Nappe $\zeta_o = (z_{MO} - h_o)/h_o$; (b) Lower Nappe $\zeta_U = z_{MU}/h_o$ [(——) Eq. (5)] for $\alpha_j = 20°$

approximately linearly, from atmospheric pressure at the free surface to the bottom pressure.

Jet Trajectories

In the following, the prismatic channel geometry is considered, and the effect of deflectors is described later. The lower and upper jet trajectories can be approximated with parabolas, as resulting for a mass point. With α_j as takeoff angle and V_j as takeoff velocity, the trajectory geometry $z(x)$ may be described for free jet flow as

$$z = z_o + \tan \alpha_j x - gx^2/(2V_j^2 \cos^2\alpha_j) \quad (3)$$

The flow depth across a flip bucket remains almost constant, and the takeoff flow depth at $x = 0$ is thus $z_o = h_o$ for the upper nappe, and $z_o = 0$ for the lower nappe, respectively. Furthermore, the takeoff velocity V_j is nearly equal to the approach velocity V_o for flow conditions without scale effects ($h_o \geq 5$ cm). Introducing the normalized coordinates relating to the upper (subscript O) nappe profile as $Z_O = (z_O - h_o)/(z_M - h_o)$ and $X = x/(h_o F_o^2)$, where z_M is the maximum (subscript M) nappe elevation above the takeoff elevation, results in

$$Z_O = \tan \alpha_j X - \frac{1}{2}\frac{X^2}{\cos^2\alpha_j} \quad (4)$$

Fig. 6(a) shows the experimental data $Z_O(X)$ for various flow configurations and produces agreement with (4) provided $\alpha_j = 20°$ is fitted. The takeoff angle α_j is thus significantly smaller than the deflection angle $\beta = 30°$, a fact also discussed by Vischer and Hager (1998).

The maximum nappe elevation can be determined from (3) to $z_M = z_o + (V_o^2/2g)\sin^2\alpha_j$; thus

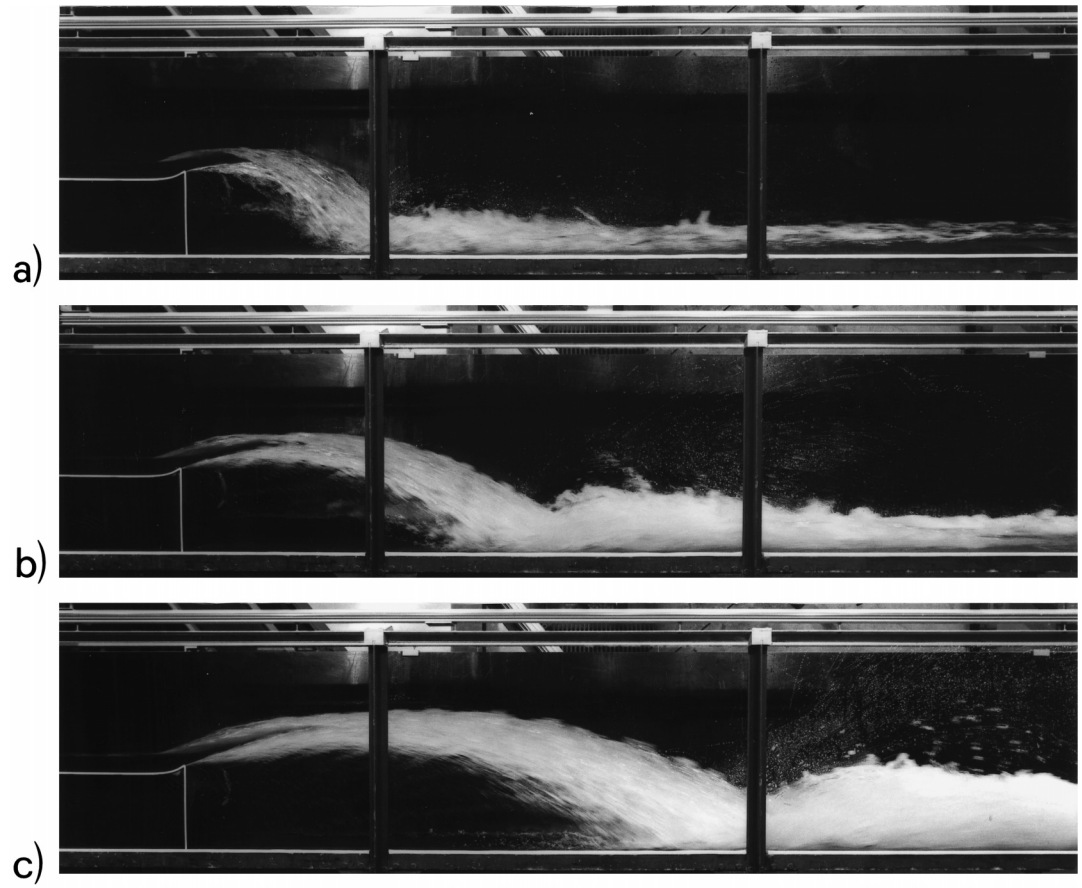

FIG. 8. Side Views to Flip-Bucket Flows with $h_o = 50$ mm: (a) $F_o = 3$; (b) $F_o = 5$; (c) $F_o = 7$

J. Hydraul. Eng. 2000.126:837-845.

$$z_M/h_o = z_o/h_o + (F_o^2/2)\sin^2\alpha_j \quad (5)$$

in agreement with the parameter choice Z and X as previously introduced.

The data for the lower (subscript U) nappe trajectory were analyzed correspondingly using $Z_U = z_U/z_M$ and $X = x/(h_o F_o^2)$. Fig. 6(b) shows agreement with (4) again, provided $\alpha_j = 20°$. The maximum of the upper and lower nappe profiles $\zeta_o = (z_{MO} - h_o)/h_o$ and $\zeta_U = z_{MU}/h_o$ as functions of F_o are plotted in Fig. 7, and one notes agreement with prediction (5) for $\alpha_j = 20°$ again. The effects of h_o/R and F_o on the takeoff angle α_j are currently not generally clarified, and indications of Vischer and Hager (1998) can be used for a preliminary estimation of the takeoff angle α_j.

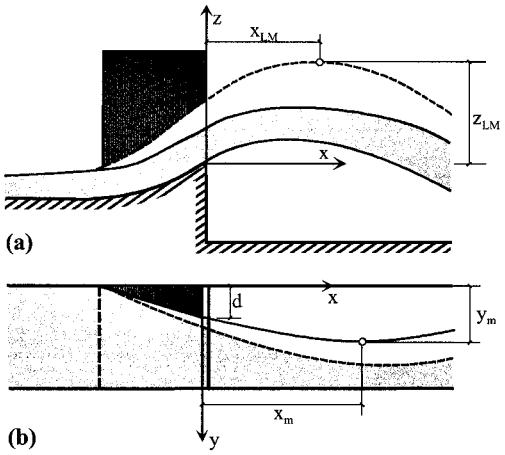

FIG. 9. Flow Pattern across Flip Bucket with Side Deflector; Plane Central Flow (Dark Area) and Shock Wave (Light Area) Regions in: (a) Side View; (b) Plan

The present data refer exclusively to the near field of nappe development, where effects of surface tension are absent. As is seen from Fig. 6, the data apply up to $X \cong 1$. Fig. 8 shows typical photographs for three flow configurations. Note the air entrainment along the upper and lower nappes starting at takeoff and advancing into the jet core. Note also the significant difference between the deflection angle β and the takeoff angle $\alpha_j < \beta$.

EFFECT OF DEFLECTORS

Fig. 9 defines the main flow features for flip buckets with a deflector. Due to the abrupt wall deflection at the bucket beginning, a shock wave is generated that is perturbed by the flip bucket and the jet deflection into the air when compared to the standard configuration in a horizontal rectangular channel (Vischer and Hager 1998). In the present context an experimental approach was selected.

Fig. 10 shows a flip bucket with a 20° deflector. The shock wave starts slightly upstream from the deflector beginning, increases strongly until its end, and expands transversally in the downstream direction. Fig. 11 shows side and corresponding plan views of flows with a 20° deflector. The maximum height of the shock wave is typically twice the height of the nonperturbed flow, and there is considerable contraction of the flow in plan. The elevation difference h_s between the approach and downstream channels was relatively small in the present setup, as is typical for bottom outlets, and a fully developed nappe could not be observed.

Tailwater views reveal a considerable effect of deflector angle φ on the jet contraction. For $\varphi = 10°$, there is hardly a

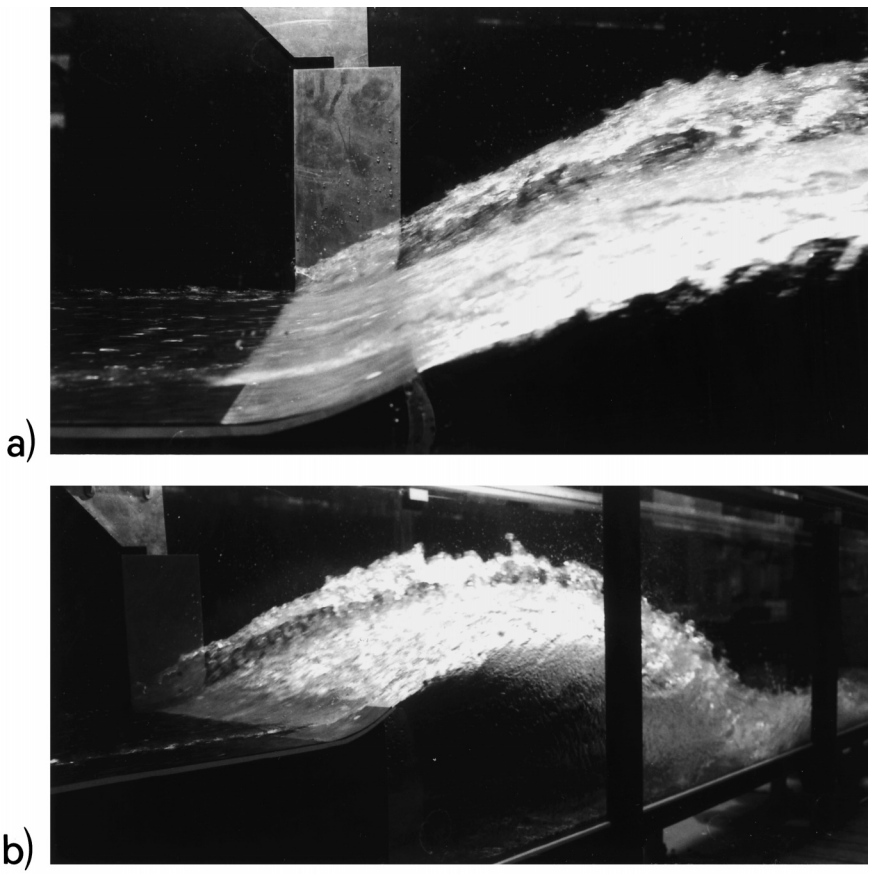

FIG. 10. Shock-Wave Development at Flip Bucket for $F_o = 5$ and $\varphi = 20°$: (a) Close to Takeoff Section; (b) View in Downstream Direction

J. Hydraul. Eng. 2000.126:837-845.

contraction, although the shock wave may be large, whereas the shock wave may expand over the entire channel width for $\varphi = 30°$ (Fig. 12).

The streamwise shock-wave profile (subscript L) resembles the lower nappe profile of a sharp-crested weir flow. The profile of the standard spillway was generalized by Hager (1987) and also considered in the present case with $X^* = A(X_L + B)$ as

$$Z_L = X^* \ln(X^*)/C - D \tag{6}$$

where $A = 0.14$; $B = 2.7$; $C = 0.023$; and $D = 16$. Furthermore, coordinates are defined as

$$X_L = x/(h_o F_o) \tag{7}$$

$$Z_L = (z_L - z_{LM})/(h_o \sin^{3/8}\varphi) \tag{8}$$

with z_{LM} = maximum nappe elevation. Fig. 13 compares the data with (6), and overall agreement is noted. When comparing (6) with (4), significantly different profiles result along the shock wave and the channel axis, as is also seen from Fig. 11.

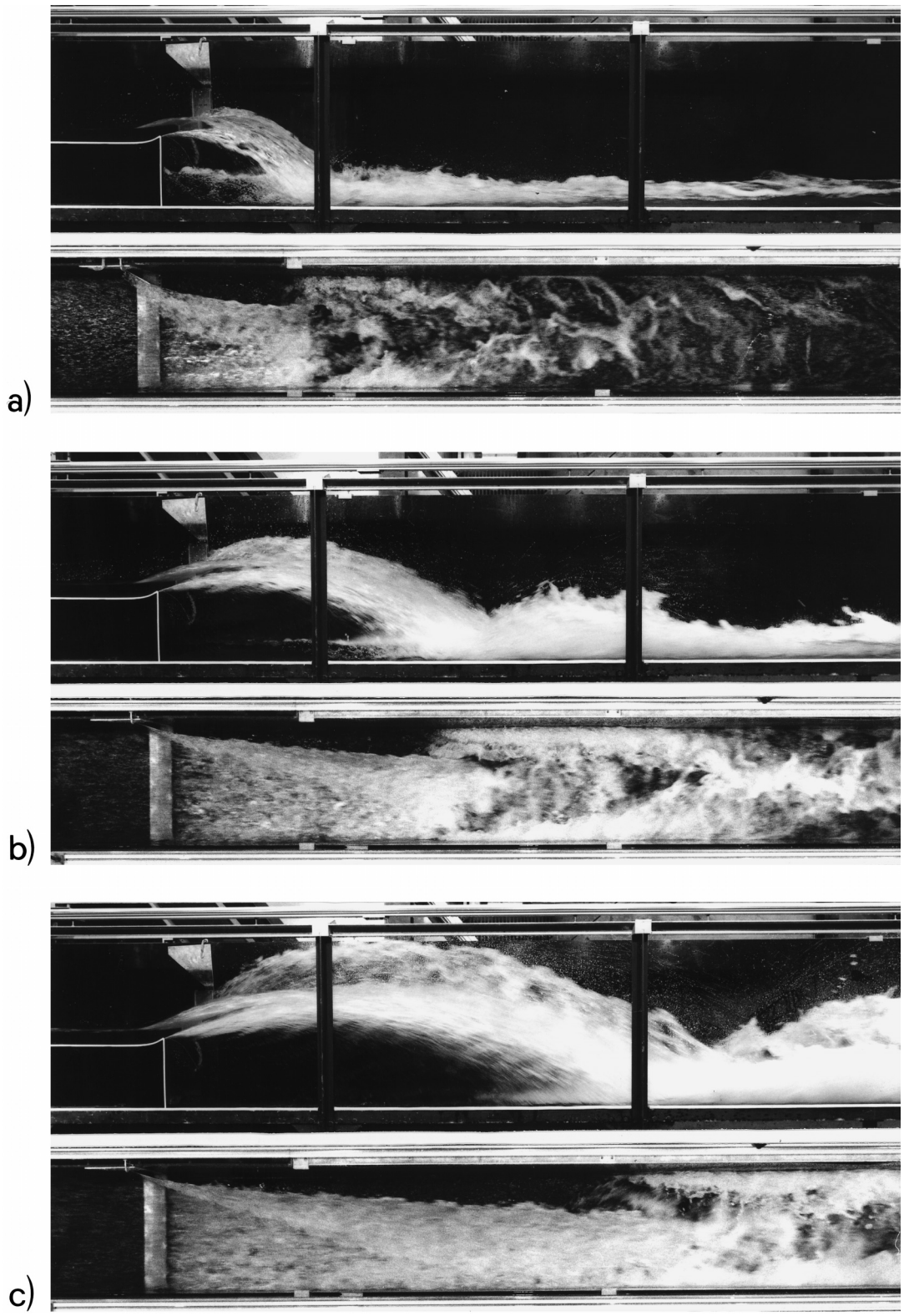

FIG. 11. Side Views and Plans for Flip Buckets with 20° Deflector and $h_o = 0.05$ m: (a) $F_o = 3$; (b) $F_o = 5$; (c) $F_o = 7$

J. Hydraul. Eng. 2000.126:837-845.

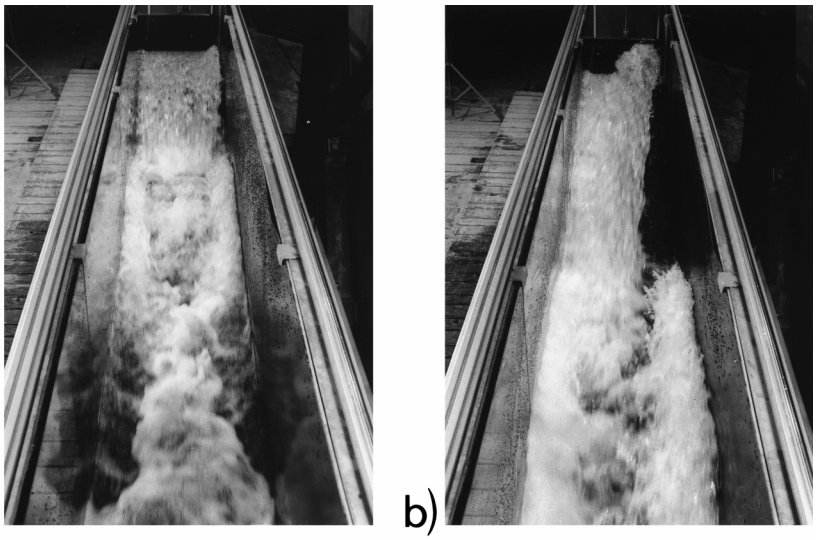

FIG. 12. Tailwater Views on Flip Bucket with Deflector for h_o = 0.05 m, F_o = 5: (a) φ = 10°; (b) φ = 30°

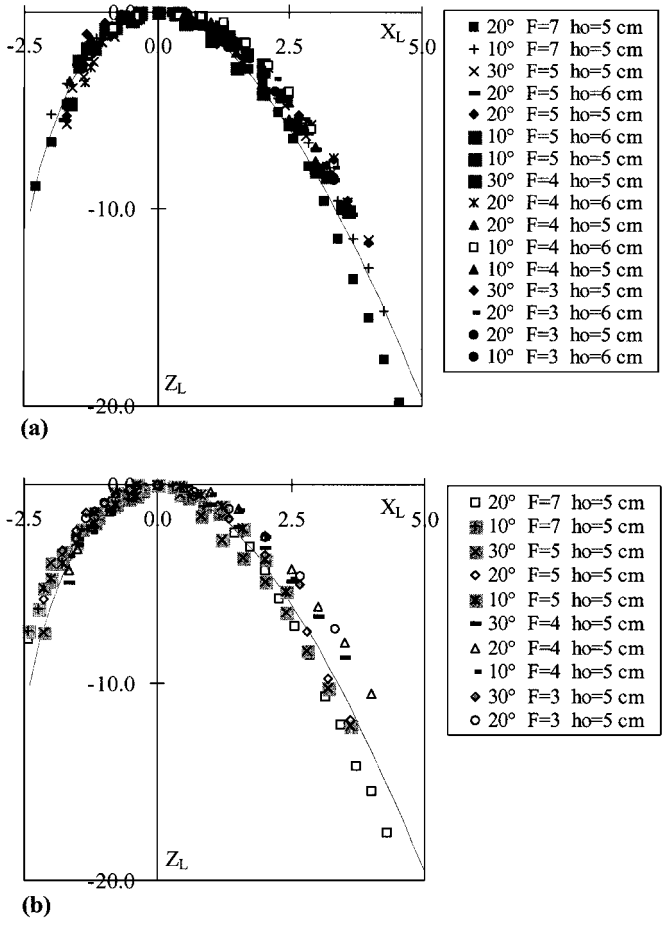

FIG. 13. Shock-Wave Profiles $Z_L(X_L)$ for: (a) R = 0.20 m; (b) R = 0.25 m [(——) Eq. (6)]

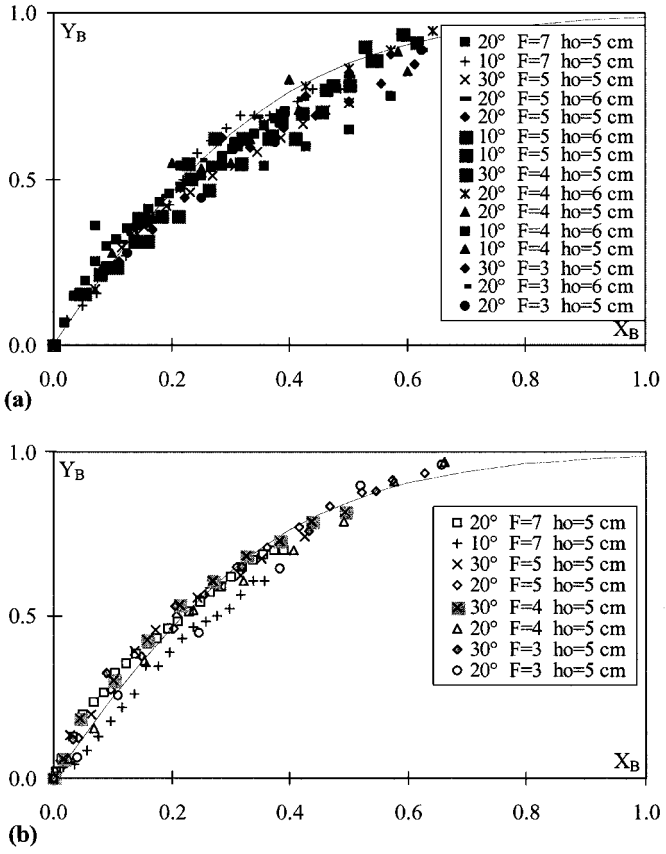

FIG. 14. Jet Width Development $Y_B(X_B)$ for: (a) R = 0.20 m; (b) R = 0.25 m [(——) Eq. (11)]

The coordinates of the profile maximum x_{LM} and z_{LM} depend exclusively on the approach Froude number F_o as

$$x_{LM}/(h_o F_o) = 0.05 F_o^2 \tag{9}$$

$$z_{LM}/(h_o \sin^{3/4}\varphi) = 0.45 F_o^2 \tag{10}$$

The streamwise decay of jet thickness $y(x)$ involves the minimum (subscript m) jet width y_m at location x_m. Introducing the normalized coordinates $X_B = x/x_m$ and $Y_B = (y - d)/(y_m - d)$, where d = deflector width (Fig. 9), yields simply an expression

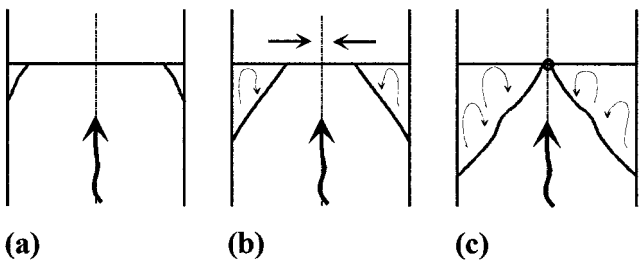

FIG. 15. Choking Flow Patterns for Flip Buckets without Deflectors: (a) Development of Lateral Wings; (b) Contraction of Central Flow Portion; (c) Incipient Choking for Critical Flow

J. Hydraul. Eng. 2000.126:837-845.

shown in Fig. 14 involving the tangent hyperbolic function tanh

$$Y_B = \tanh X_B^{2.5} \tag{11}$$

with the effects of φ, F_o, and h_o contained in the normalizing parameters x_m and y_m

$$x_m/(h_o \sin^{0.25}\varphi) = 4F_o^2 \tag{12}$$

$$y_m/(h_o \sin^2\varphi) = 5F_o^2 \tag{13}$$

Thus x_m and y_m depend quadratically on the approach Froude number F_o, and y_m depends significantly on the deflector angle. Although $\varphi = 10°$ corresponds to a relatively small angle, $\varphi = 30°$ may be considered an upper limit because of strong jet deformation. Then the shock wave is extremely high, and the impact on the tailwater bed is concentrated. Another important implication is discussed in the following section.

FLOW CHOKING

Description

Supercritical flow breaks down once the local Froude number is sufficiently close to 1 (i.e., critical flow). Any perturbation of supercritical flow such as a bed elevation, a curve, or a contraction may initiate choking. Thus dealing with supercritical flows always demands determination of choking conditions. If a supercritical flow chokes, the resulting flow conditions change significantly, and it is important to know the limit conditions under which supercritical flow can no longer be maintained. Also, a distinction has to be made between flip buckets with and without the presence of a deflector.

If the approach Froude number F_o is steadily reduced for a flip bucket without a deflector, a condition with lateral wings results where the flow in the bucket recirculates [Fig. 15(a)], due to the turbulent velocity distribution. Accordingly, the forward flow undergoes some contraction. Further reducing F_o results in an increased flow contraction [Fig. 15(b)] to the point where the two recirculating fronts match at the axis of the takeoff section [Fig. 15(c)]. Observations indicate that the corresponding axial flow depth is nearly equal to the critical flow depth $h_c = (Q^2/gb^2)^{1/3}$ and that the local Froude number is $F = 1$. Once this condition has occurred, the supercritical approach flow breaks down, and a hydraulic jump results upstream from the bucket. The overflow jet is then not discharged into the downstream channel, but it impinges at the base of the flip bucket, with an increased potential of erosion. To return to supercritical approach flow, a much larger approach Froude number is required than for incipient choking (Vischer and Hager 1998). Blowout flow is not considered here because structures should be designed and operated far beyond incipient choking.

For flip buckets with a deflector, the flow pattern during a reduction of approach Froude number is similar, except that inception is reached asymmetrically because of the additional formation of a shock wave close to the deflector (Fig. 16).

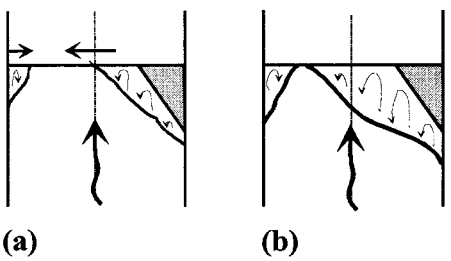

FIG. 16. Choking Flow Patterns for Flip Buckets with Deflector: (a) Combined Effects of Recirculation and Shock-Wave Formation; (b) Asymmetric Inception of Choking

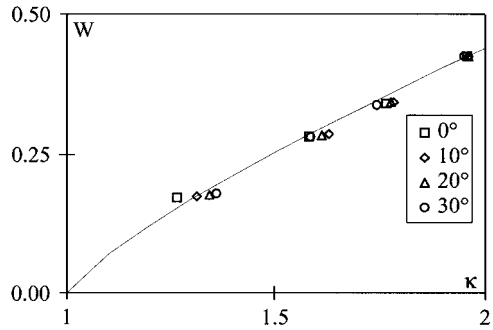

FIG. 17. Incipient Choking for Flip Bucket with Deflection Angles $0 < \varphi \cdot 30°$ [(——) Eq. (14)]

Here, the condition of critical flow could not be verified experimentally, also due to the complex surface pattern close to choking inception. In the present case, choking was defined as the condition under which the two fronts meet at the takeoff section. Any further reduction of F_o resulted in immediate and total breakdown of approach flow.

Choking Criterion

A computation of choking involves critical flow with complex pressure distributions on the flip bucket and in the overflow jet, as well as highly nonuniform velocity distributions that are not amenable for a basic hydraulic computation. The main parameters are the relative bucket height $W = w/h_o$, the deflector angle φ, and the incipient (subscript i) approach Froude number F_{oi}. Fig. 17 shows a generalized design diagram based on the combined parameter $\kappa = (\cos\varphi)^{2.5}F_{oi}$ as a function of relative bucket height W. The data may be expressed as

$$W = 0.44(\kappa - 1)^{0.8} \tag{14}$$

For a certain deflector geometry φ and bucket height W, a minimum approach Froude number is thus required to inhibit choking ($F_o > 1$). Eq. (14) is valid, as are all of the other results, but only for free jet flow, for which the tailwater effect is absent. For $\varphi \leq 30°$, one may develop $\cos^{2.5}\varphi = [1 - (1/2)\varphi^2]^{2.5} \cong 1 - (5/4)\varphi^2$ and $\cos^{-2.5}\varphi = 1 + (5/4)\varphi^2$, such that

$$F_{oi} = 1 + \left(\frac{9}{4}W\right)^{5/4} + \frac{5}{4}\varphi^2 \tag{15}$$

Eq. (15) demonstrates that for a ''horizontal'' ($W = 0$) bucket without deflector ($\varphi = 0$) the incipient Froude number is $F_{oi} = 1$. Increasing W has an almost linear effect on F_{oi}, whereas the effect of the deflector is quadratic. Typically, W is of the order 1, and the minimum approach Froude number according to (15) must be 3.76. For a deflector of $\varphi = 10°$ and 30° (i.e., $\varphi = 0.175$ and 0.524 in rad, respectively), one has $F_{oi} = 3.80$ and 4.10, respectively. For such a large value of W, the effect of φ is relatively small.

The effect of φ is large relative to the maximum height of the shock wave, however. For $F_o = 5$, (10) gives, for $\varphi = 10°$ and 30°, respectively, $z_{LM}/h_o = 0.45 \sin^{3/4}\varphi F_o^2$ (i.e., $z_{LM}/h_o = 3.03$ and 6.69). The latter value is thus more than double the value of z_{LM}/h_o for 10°. For a bucket without deflector, and $\alpha_j = 20°$ as previously established, one has $z_{LM}/h_o = 1.46$, which is half of the height of the 10° deflector bucket.

CONCLUSIONS

Flip buckets with a deflector have received minor attention, although thousands of those structures exist worldwide. The present experimental study intends to add useful design information for bucket flow, mainly when used downstream of a bottom outlet.

J. Hydraul. Eng. 2000.126:837-845.

For flip buckets without a deflector, the following information is now available:

- Bottom pressure distribution
- Lower and upper near field nappe trajectories
- Coordinates of maximum jet elevation

The radius of the bucket has a relatively small effect on bucket flow. However, the takeoff angle was demonstrated to be significantly different from the deflection angle and determines the parabolic jet trajectory close to the bucket. For the 30° bucket geometry presently considered, all of the data followed a takeoff angle $\alpha_j = 20°$.

For flip buckets with a deflector, the deflector angle φ is an important design quantity in terms of the following:

- Shock-wave profile in plan and section
- Maximum height of shock wave
- Maximum jet contraction
- Choking flow condition

A deflector is a simple design element to deflect the flow, without problems regarding cavitation damage. A significant disadvantage of the bucket is the increased level of choking inception, and this effect has to be carefully checked. Damages mainly due to erosion downstream of the bucket and choking of an upstream bottom outlet tunnel may result otherwise. Also, a flip bucket with a deflector may enhance spray formation that can result in adverse effects on a certain design.

ACKNOWLEDGMENTS

The writers would like to acknowledge the steady interest in this work by Prof. Dr. H.-E. Minor, director of VAW, Zurich. The writers would also like to thank Olivier Baud for his assistance during the early stage of the project.

APPENDIX I. REFERENCES

Auroy, F. (1951). ''Les évacuateurs de crues du barrage de Chastang.'' *Proc., 4th ICOLD Congr.*, Vol. Q12, R82, 661-686 (in French).
Balloffet, A. (1961). ''Pressures on spillway flip buckets.'' *J. Hydr. Div.*, ASCE, 87(5), 87–98.
Chen, T.-C., and Yu, Y.-S. (1965). ''Pressure distribution on spillway flip buckets.'' *J. Hydr. Div.*, ASCE, 91(2), 51–63.
Coyne, A. (1944). ''Prototypes modernes de barrages et d'usines hydro-électriques.'' *Travaux*, 28, 25–29 (in French).
Coyne, A. (1951). ''Observations sur les déversoirs en saut de ski.'' *Proc., 4th ICOLD Congr.*, Vol. Q12, R89, 737–756 (in French).
Godon, R. (1936). ''Le barrage et l'usine hydro-électrique de Marèges, sur la Dordogne.'' *Techniques des Travaux*, 12, 101–110 (in French).
Gong, Z., Liu, S., Xia, S., and Lin, B. (1987). ''Flaring gate piers.'' *Design of hydraulic structures*, A. R. Kia and M. L. Albertson, eds., Colorado State University, Fort Collins, Colo., 139–146.
Hager, W. H. (1987). ''Continuous crest profile for standard spillway.'' *J. Hydr. Engrg.*, ASCE, 113(11), 1453–1457.
Henderson, F. M., and Tierney, D. G. (1963). ''Flow at the toe of a spillway.'' *La Houille Blanche*, Grenoble, France, 18(1), 42–50.
Lenau, C. W., and Cassidy, J. J. (1969). ''Flow through spillway flip bucket.'' *J. Hydr. Div.*, ASCE, 95(5), 633–648.
Maitre, R., and Obolensky, S. (1954). ''Etude de quelques caractéristiques de l'écoulement dans la partie aval des évacuateurs de surface.'' *La Houille Blanche*, Grenoble, France, 9(7), 481–511 (in French).
Mason, P. J. (1993). ''Practical guidelines for the design of flip buckets and plunge pools.'' *Water Power and Dam Constr.*, U.K., 45(9), 40–45.
Peterka, A. J. (1983). *Hydraulic design of stilling basins and energy dissipators*, 7th Ed., *Engrg. Monograph 25*, Bureau of Reclamation, U.S. Department of the Interior, Denver.
Rajan, B. H., and Shivashankara Rao, K. N. (1980). ''Design of trajectory buckets.'' *Irrig. and Power*, India, 37(1), 63–76.
Reinauer, R. (1995). ''Kanalkontraktion bei schiessendem Abfluss und Stosswellenreduktion mit Diffraktoren.'' PhD thesis 11320, Eidgenössische Technische Hochschule, Zurich (in German).
Rhone, T. J., and Peterka, A. J. (1959). ''Improved tunnel spillway flip buckets.'' *J. Hydr. Div.*, ASCE, 85(12), 53–76.
Schwalt, M. (1994). ''Vereinigung schiessender Abflüsse.'' PhD thesis 10370, Eidgenössische Technische Hochschule, Zurich (in German).
Vischer, D. L., and Hager, W. H. (1995). *Energy dissipators*, *IAHR Hydr. Struct. Des. Manual 9*, Balkema, Rotterdam, The Netherlands.
Vischer, D. L., and Hager, W. H. (1998). *Dam hydraulics*, Wiley, Chichester, England, and New York.
Zhenlin, D., Lizhong, N., and Longde, M. (1988). ''Some hydraulic problems of slit-type buckets.'' *Proc., Int. Symp. on Hydr. for High Dams*, 287–294.

APPENDIX II. NOTATION

The following symbols are used in this paper:

B = bend number;
b = channel width;
d = deflector width;
F = Froude number;
g = gravitational acceleration;
H_p = normalized pressure head;
h = flow depth;
h_P = pressure head;
h_s = drop height;
Q = discharge;
R = radius of curvature;
V = average cross-sectional velocity;
W = relative bucket height;
w = bucket height;
X = $x/(h_o\mathsf{F}_o^2)$ normalized streamwise coordinate;
X' = x/h_o;
x = streamwise coordinate;
Y = normalized transverse coordinate;
y = jet thickness;
Z = normalized vertical coordinate;
z = vertical coordinate;
α_j = takeoff angle;
β = deflection angle;
ζ = relative jet extrema;
κ = choking parameter;
σ = fitting parameter; and
φ = deflector angle.

Subscripts

B = thickness of jet;
c = critical flow;
i = incipient choking;
j = jet takeoff;
L = shock profile;
M = maximum;
m = minimum;
O = upper trajectory;
o = approach;
P = pressure head; and
U = lower trajectory.

J. Hydraul. Eng. 2000.126:837-845.